Urol Res (1984) 12:135–141

Urological Research
© Springer-Verlag 1984

Distribution of Concanavalin A Binding Sites on Normal Human Urinary Bladder Mucosa and Bladder Tumors by Transmission and Scanning Electron Microscopy and X-Ray Microanalysis

H. Takayama

Department of Urology, Shiga University of Medical Science, Otsu, Japan

Accepted: November 22, 1983

Summary. We used concanavalin A (con A)-peroxidase-iron dextran-diaminobenzidine (DAB) technique for the electron microscopic detection of con A binding sites on cell membranes. Normal bladder mucosa showed a sparse distribution of con A binding sites with both transmission (TEM) and scanning (SEM) electron microscopy, but bladder tumors showed a higher concentration in the distribution of con A binding sites in proportion to the histopathological grade of transitional cell carcinoma. Quantitative estimation of the con A binding sites was attempted using scanning X-ray pulse analysis of iron elements contained in the reaction complexes. Con A binding sites were quantitatively the smallest in normal mucosa, increasing proportionate to the grade of the bladder tumor. Some specimens were compared by the ferritin-labelled method and the pattern of ferritin conjugates distribution was similar to that seen with the con A-peroxidase-iron dextran method.

Key words: Concanavalin A, Lectin receptors, Bladder tumor, Electron microscopy, X-ray microanalysis.

Introduction

It is becoming apparent that the presence of carbohydrate residues on the cell surface may be of importance in the regulation of growth and morphogenesis. These carbohydrate residues specifically bind various plant lectins, such as con A, a jack bean protein, which reacts with α-D-mannosides, α-D-glucosides or β-D-fructosides [10]. Labelled lectins can be used as reagents for studying the changes in the specific carbohydrates groups on cell membranes.

Several methods for ultrastructural demonstration of con A binding sites have been reported [25], but there are only a few methods which permit visualization of con A binding sites by both SEM and TEM.

Con A-peroxidase-DAB complexes [5], con A-haemocyanin complexes [23, 27] or con A-peroxidase-iron dextran-DAB complexes [2] have been reported to be substances which can be visualized by both SEM and TEM. The method of Bacetti et al. [2], using electron probe X-ray microanalysis, has demonstrated the quantitative detection of con A binding sites. Little consideration by using these methods has been given to the bladder mucosa and tumor. The present study reports the results obtained with a method which permits visualization of con A binding sites by both TEM and SEM. Of special interest were the studies with X-ray microanalysis that enabled us to quantitatively measure the distribution and the density of con A binding sites on the surface of bladder mucosa and tumor of various grades.

The advantage of the present study is that the distribution of con A binding sites is shown as a simultaneous morphological ultrastructure and an X-ray pulse from signals of binding iron particles.

Materials and Methods

Four specimens of normal bladder mucosa for control study were obtained from the patients who had a prostatectomy for benign prostate hyperplasia without urinary tract infection and from the histologically normal portion of a bladder after a total cystectomy. Fourteen specimens of bladder tumors were obtained after total cystectomy or a transurethral resection, and all of those showing transitional cell carcinoma were used in this study. Treatment of the specimens was performed in the following steps (modified method from Bacetti et al. [2]): 1) washing of the material surface in 0.01 M phosphate-buffered saline (PBS) ($NaH_2PO_4 \cdot 2H_2O$ 0.45 g, $Na_2HPO_4 \cdot 12H_2O$ 3.23 g and NaCl 8.0 g/l, pH 7.2; 2) fixation in 2.5% glutaraldehyde in PBS for 1 h at 4 °C; 3) rinsing PBS; 4) incubation in 100 μg/ml con A in PBS for 30 min at room temperature; 5) rinsing in PBS; 6) incubation in 50 μg/ml horseradish peroxidase and 12.5 mg/ml iron dextran for 30 min at room temperature; 7) washing in PBS; 8) fixation in 2.5% glutaraldehyde in PBS for 30 min at 4 °C; 9) rinsing in PBS; 10) DAB reaction for 30 min at room temperature; 11) rinsing in PBS; 12) postfixation in 1% OsO_4 in PBS for 1 h at 4 °C; 13) dehydration through a graded series of ethanol solutions.

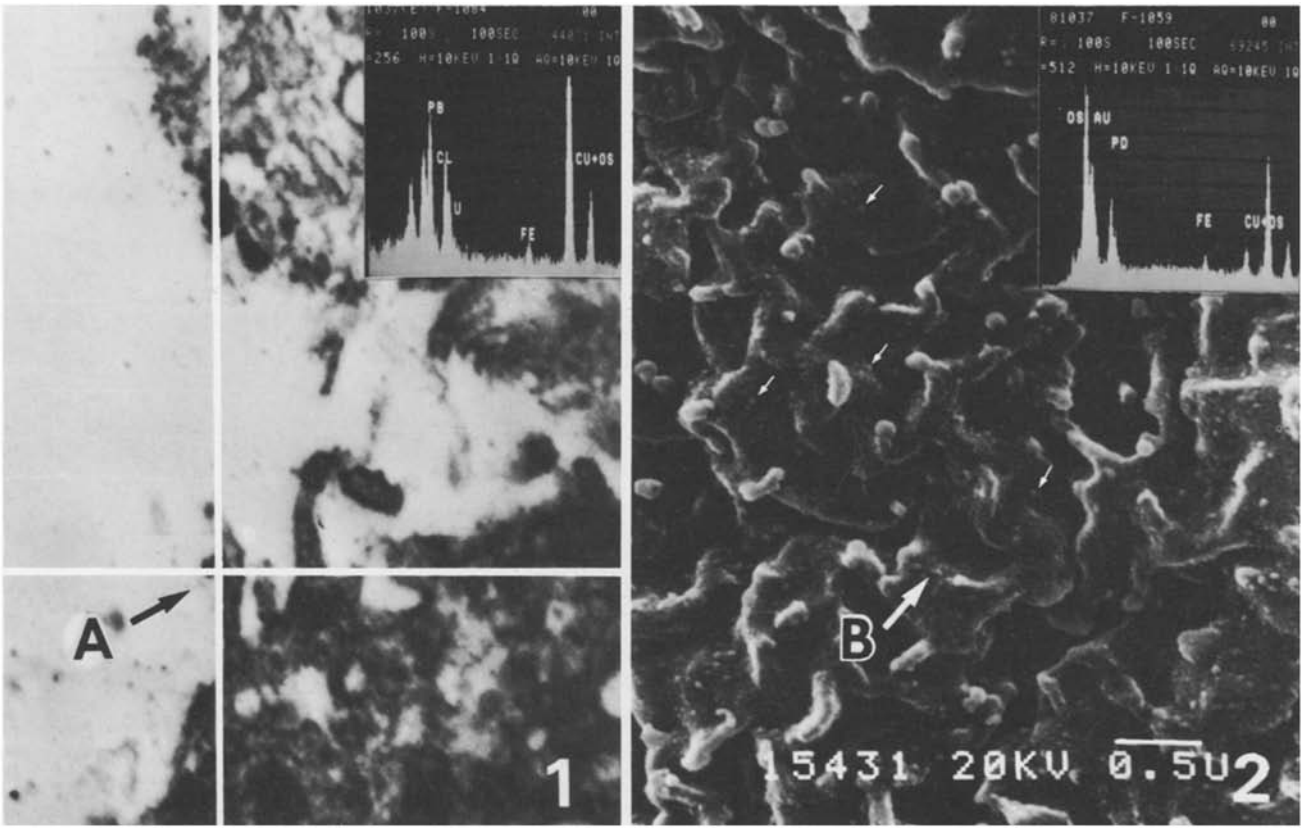

Fig. 1. Scanning transmission electron micrograph of grade III tumor. Spot X-ray microanalysis on the reaction product (point A) shows an iron peak (*Inset*). (Stained with uranyl nitrate and lead citrate) x24,000

Fig. 2. SEM picture of normal bladder mucosa showing a dispersed distribution of reaction products, some of which were pointed by *arrows*. x23,000. *Inset:* Spot X-ray microanalysis of one prominence (*point B*) shows an iron signal peak

The control preparation for specificity of the reaction was treated by adding 0.2 M α-methyl-D-mannoside to the con A solution at step 4).

For TEM the dehydrated specimens were embedded in Epon and sectioned. Thin sections were placed on carbon-coated copper grids and observed unstained or stained with uranyl nitrate and lead citrate in a Hitachi H-500 or H-700 electron microscope equipped with an energy dispersive X-ray spectrometer. Some specimens were compared by the ferritin-labelled method to investigate whether this detection method of con A binding sites was reliable. Ferritin-labelled con A was purchased from E·Y Lab. Inc. (USA) and certified to show a single band by disc gel electrophoresis.

For SEM the dehydrated specimens were dried in a critical point drying apparatus, mounted on aluminum specimen holders, coated with gold-palladium and observed in a Hitachi HFs-2S or S-450 scanning electron microscope.

For electron probe X-ray microanalysis, block specimens were examined by spot analysis and X-ray mapping in a Hitachi X-650 scanning microanalyzer. In addition, iron signals with scanning pulse analysis, done for five different areas (1,000 magnifications) and consisting of several cells on each specimen, were calculated by a computer at 20 KV of accelerating voltage, 38.0 degree of effective take-off angle and 200 s of total analysis time.

Results

With TEM con A-peroxidase-iron dextran-DAB reaction complexes were found to consist of aggregates of irregular electron dense precipitates containing fine dense particles on the cell membrane. With SEM the reaction products showed granular prominences of about 50–80 nm in diameter on the cell surface, whereas the specimen in the control experiment lacked those granular prominences. The X-ray spot analysis revealed an iron signal just on the dense aggregates seen in the transmission micrograph (Fig. 1, Inset) and on the granular prominence in the scanning micrograph (Fig. 2, Inset). These observations demonstrate that the aggregates of fine dense particles in the transmission micrograph are iron particles and the granular prominences in the scanning micrograph contain iron particles. These aggregates and granular prominences indicate the reaction product of con A-peroxidase-iron dextran-DAB treatment, namely, the con A binding sites.

TEM for cell membranes of normal bladder mucosa showed smooth surfaces with microridges and a few short microvilli. Con A binding aggregates were discontinuously found on the smooth membranes and microridges (Fig. 3).

With SEM the luminal surface cells of normal bladder mucosa were pentagonal or hexogonal and their cell boundaries were well defined with a slightly elevated line consisting of short microvilli. The majority of the cells had a network of randomly arranged microridges. Con A binding

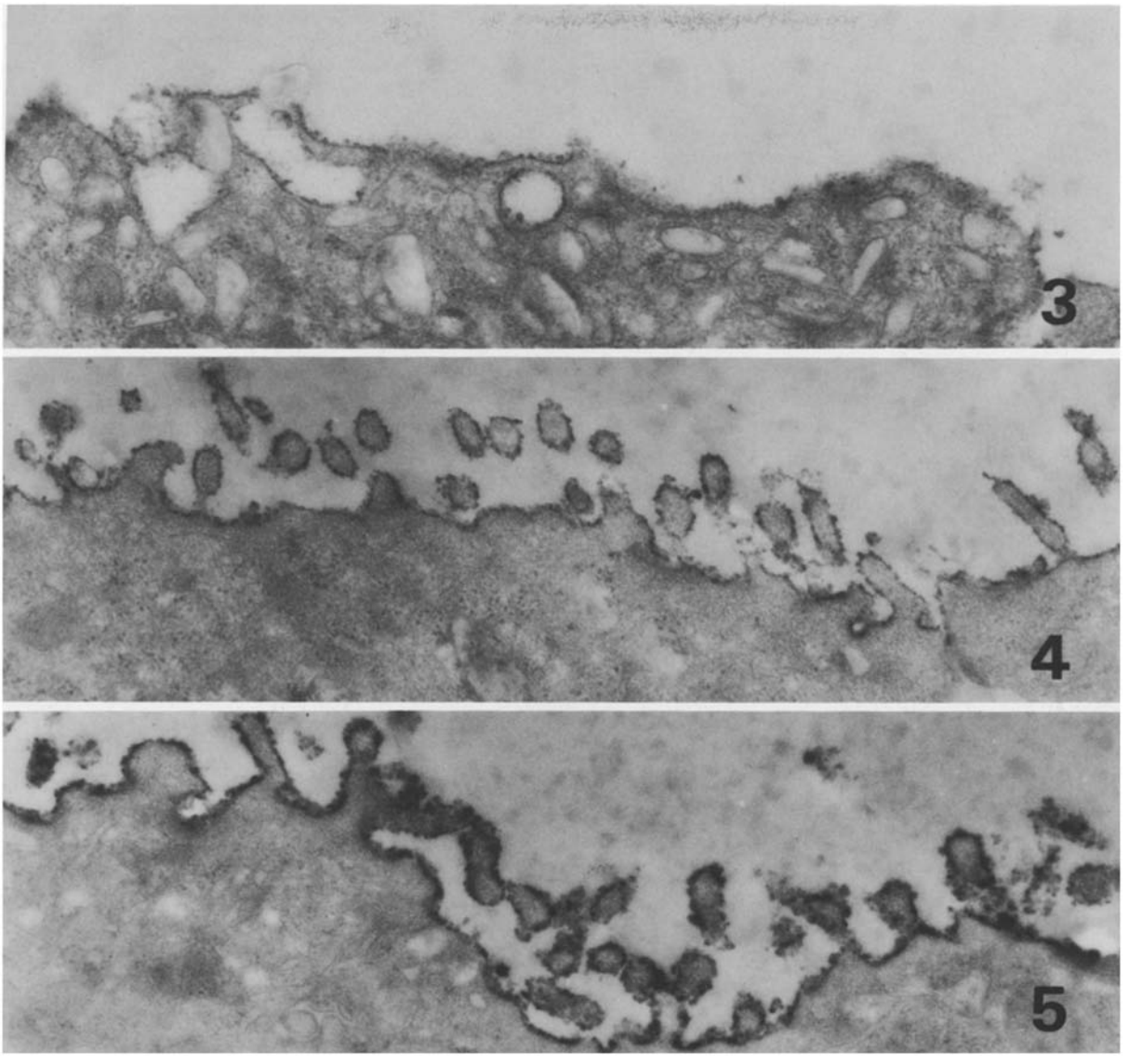

Fig. 3. TEM picture showing sparse and discontinuous deposition of reaction product over the cell membrane of normal mucosa. (Stained with uranyl nitrate only) x35,000

Fig. 4. TEM picture of grade I tumor. Deposition of reaction product over the cell membrane is denser than the normal mucosa but it is discontinuously distributed. (Stained with uranyl nitrate only) x35,000

Fig. 5. TEM picture of grade III tumor. The continuous and dense distribution of reactive complexes is seen throughout the entire cell membrane and microvilli. (Stained with uranyl nitrate only) x35,000

prominences were seen on nearly the entire area of the cell surface and microridges but the distribution was sparse and random (Fig. 2).

Bladder tumors were examined according to the pathohistological grading of cell differentiation from grade I to III.

With TEM the cell membrane in grade I tumors appeared to have a relatively smooth surface with short microvilli. Deposition of reactive products on the membranes was discontinuously distributed and slightly increased compared to the normal mucosa (Fig. 4). As the grade of the tumor malignancy increased, the cell membranes showed a proportionally more irregular surface with longer pleomorphic microvilli. Reaction products also increased proportionally to the grade and in grade III they were abundant, showing an almost continuous layer of electron dense aggregates over the cell membrane and microvilli (Fig. 5).

The pattern of ferritin conjugate distribution on normal bladder mucosa (Fig. 6) and bladder tumor (Fig. 7) was similar to that seen with the con A-peroxidase-iron dextran method, although ferritin particles were fewer in number than con A aggregates. The experiment using the ferritin labelled method demonstrated that the results in con A-peroxidase-iron dextran-DAB reaction were specific.

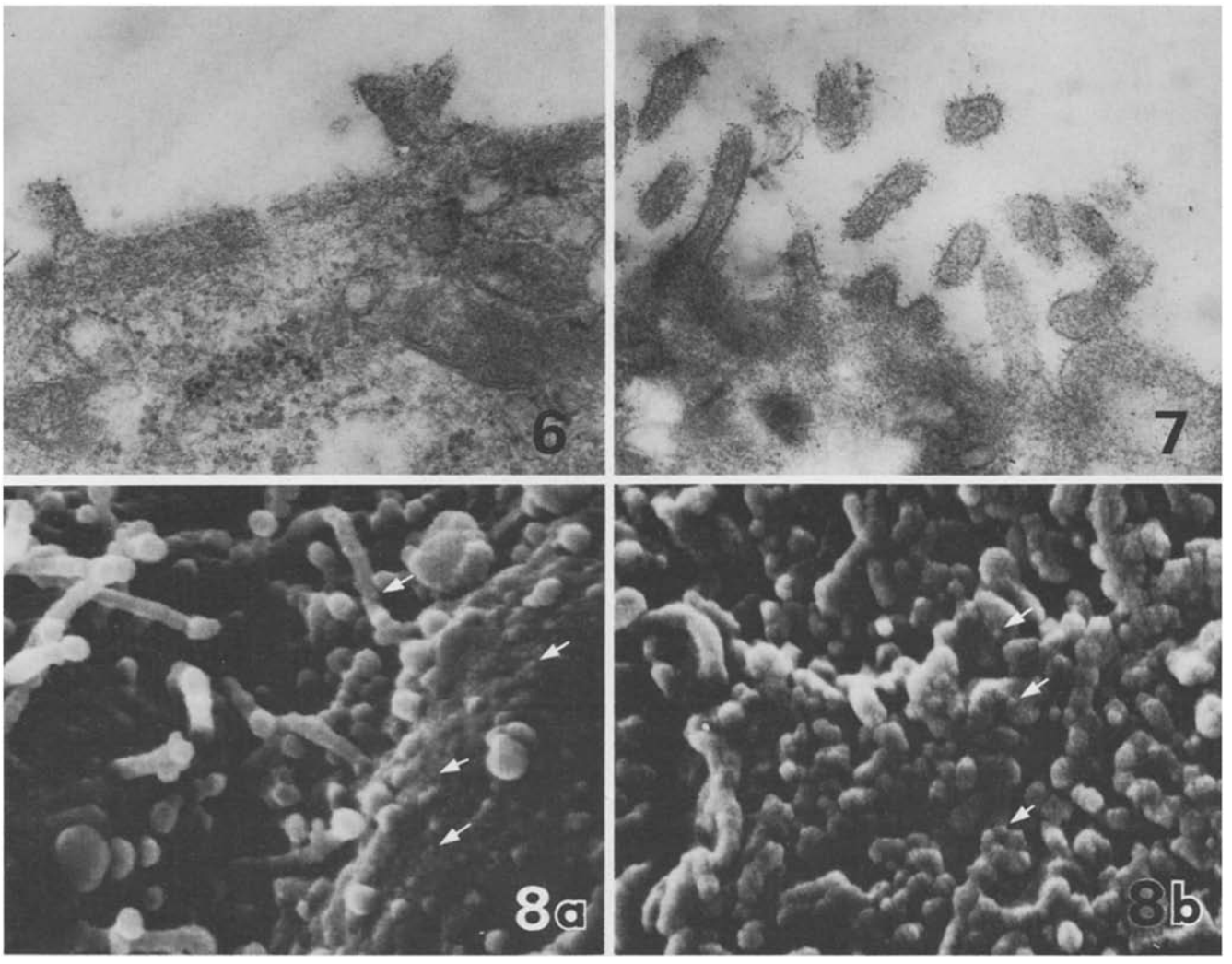

Fig. 6. TEM picture of normal mucosa treated with ferritin conjugated con A. Only a few ferritin particles are seen on the cell surface. (Stained with uranyl nitrate only) x50,000

Fig. 7. TEM picture of grade III tumor treated with ferritin conjugated con A. Dense and invariable distribution of ferritin particles is seen on the cell membrane and microvilli. (Stained with uranyl nitrate only) x50,000

Fig. 8a, b. SEM picture of grade III tumor. **(a)** Tumor cells showing long pleomorphic microvilli and nodular protrusions on their surfaces. x27,000. **(b)** Tumor cell having abundant microvilli. x27,000. Many granular prominences (some of them are shown by *arrows*) of reaction products are densely present on all regions of cell membranes and microvilli in both **(a)** and **(b)** pictures

With SEM, surface cells in grade I tumor had short microvilli and microridges on convex cell membranes, and microvilli showed a tendency of thicker density around the cell boundaries. Con A binding prominences were randomly seen on almost the entire area of cell surfaces and on each microvillus, but those distributions were not dense (Fig. 9). With progression of tumor grade, the cell surfaces varied from cell to cell. Generally, microridges seen on the normal cells disappeared, microvilli increased in number and became pleomorphic. Irregular nodular protrusions mixed with microvilli often covered the cell surfaces. In grade III tumors, some cell surfaces were covered with many pleomorphic and sometimes branched microvilli, and some had irregular nodular protrusion mixed with long microvilli (Fig. 8a). Con A binding prominences were increased in proportion to the tumor grade and those in grade III tumor were uniformly seen on all surfaces regardless of the shape: microvilli, flat or nodular protruding membranes (Fig. 8b). The distribution of the reaction products was so dense that those prominences were attached to each other in some part of the cells but they did not show clustering or patching.

Scanning X-ray pulse analysis was performed to quantitatively estimate both the con A binding sites on normal bladder mucosa and on bladder tumors from grades I to III. Counts of iron signals from cell surfaces were the smallest in the normal mucosa, increasing proportionate to the grade of the bladder tumor. The results of the scanning X-

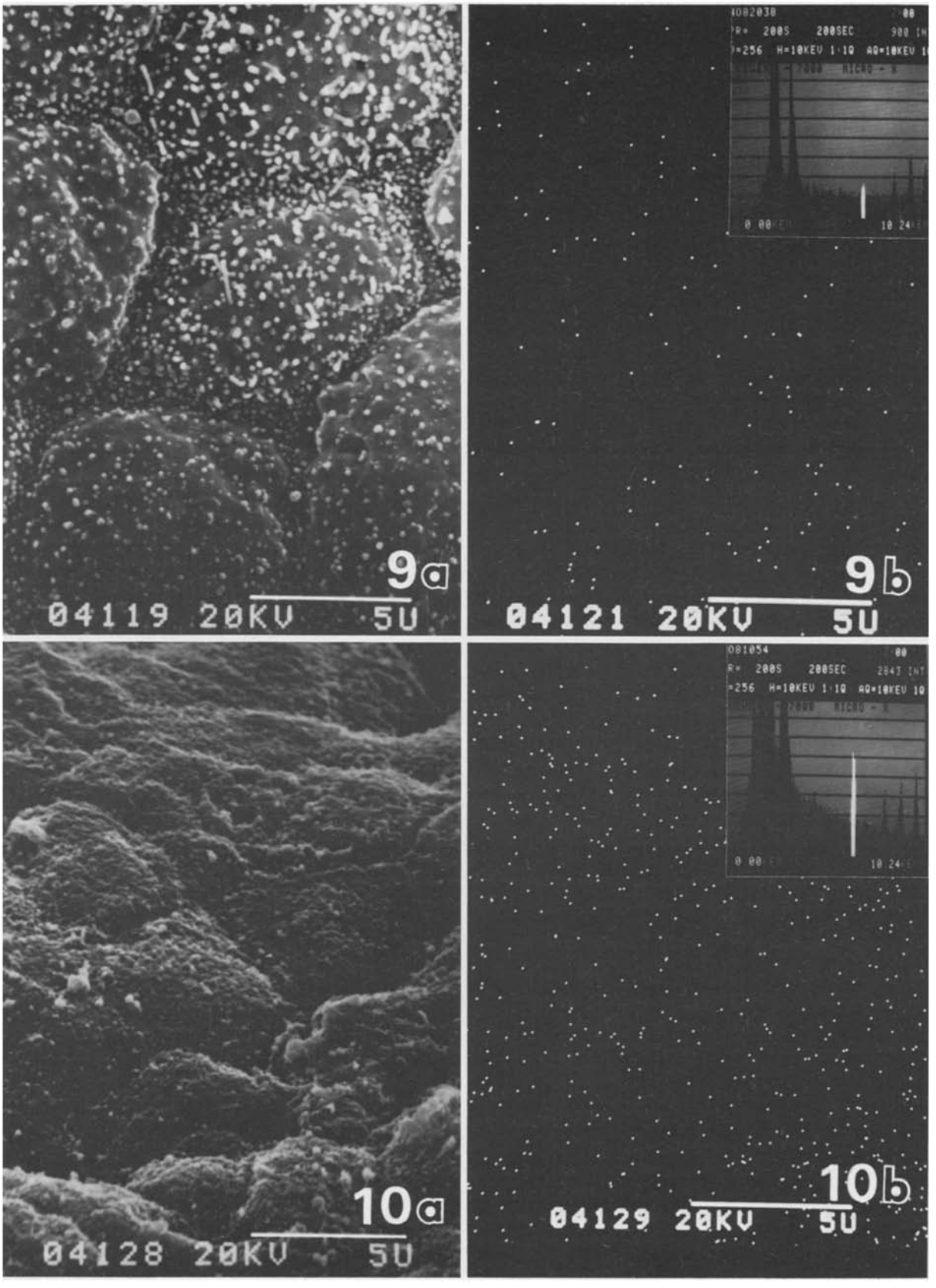

Fig. 9a, b. SEM picture and X-ray mapping showing the density of con A binding sites. (**a**) SEM picture of grade I tumor. x14,000. (**b**) X-ray mapping of iron over the same area as the 9a picture. x14,000. *Inset*: X-ray microanalysis detected at the same time. White spectrum shows an iron signal

Fig. 10a, b. (**a**) SEM picture of grade III tumor. x14,000. (**b**) X-ray mapping of iron over the same area as the 10a picture. Note the denser distribution of spots than that of grade I tumor in Fig. 9b. x14,000. *Inset*: X-ray microanalysis shows a higher spectrum of iron signals than that of grade I tumor

Table 1. Counts of iron signals with scanning pulse analysis, done for five different areas of bladder surface and consisting of several cells on each specimen, were calculated and their mean values were tabled. Iron counts are the smallest in the normal mucosa and increase proportionate to the grade of the tumor, but the statistical significance is shown as the table

Results of scanning X-ray pulse analysis	No. of cases	Mean ± S.E. (counts/s)
Normal mucosa (NM)	4	2.472 ± 0.790
Grade I tumor (GI)	4	6.131 ± 1.722
Grade II tumor (GII)	5	12.38 ± 1.071
Grade III tumor (GIII)	5	25.23 ± 4.167
Statistical significance		
Between NM and GI	$t = 2.365$	$p > 0.05$
Between GI and GII	$t = 3.010$	$p < 0.02$
Between GII and GIII	$t = 3.537$	$p < 0.01$

ray pulse analysis are summarized in Table 1. Statistical significance by Student's t test, though not seen between the normal mucosa and the grade I tumors ($p > 0.05$), was seen between the grade I and the grade II tumors ($p < 0.02$) and between the grade II and the grade III tumors ($p < 0.01$). X-ray mapping of iron over grade I tumors and grade III tumors were compared for better comprehension of the distribution of iron particles (Figs. 9 and 10). Distribution of X-ray spots was sparse in grade I tumors, but was denser in grade III tumors. X-ray microanalysis performed at the same time showed a short spectrum in grade I tumors and a higher one in grade III tumors.

Discussion

Since first reported by Bernhard [4], electron microscopy has been widely applied for visualizing con A binding sites on the cell membrane. One of the methods which enables us to obtain both a two- and three- dimensional view of the con A binding sites in the same procedure was reported by Bretton et al. [5]; in addition, they proposed the quantitative measurement of con A binding sites on SEM based on observation of distribution of con A-peroxidase-DAB complexes on the cell membranes. In this method, however, quantitative estimation cannot be expressed by a numerical value. X-ray microanalysis of iron signal from con A-peroxidase-iron dextran DAB treated rat spermatozoa has revealed a significant difference between the head and tail [2]. The use of electron probe X-ray microanalysis seems to be suitable for quantitative analysis of con A binding sites. The present study also confirmed the usefulness of scanning X-ray pulse analysis for the quantitative estimation. A previously described technique using iron dextran for visualizing con A binding sites by TEM indicated that iron dextran did not bind to the membrane surface non-specifically in the absence of con A [18]. Therefore, the method using iron dextran or peroxidase-iron dextran-DAB for detecting con A binding sites can be considered confidential.

It should, however, be noted that the number and distribution of the con A binding sites on the surface of cells is influenced by the experimental conditions; prefixation and non-fixation of the cells by glutaraldehyde showed different densities and distributions of con A binding sites. The reacting of the cells with con A at 0 °C resulted in less detectable lectin on the cell surface than at the room temperature [23]. In the present study, therefore, the chemical reaction for detecting con A binding sites was performed under the same condition in all specimens.

The remarkable difference in lectin agglutinability between normal and transformed cells has stimulated a great deal of investigation into the molecular basis of this phenomenon. Many studies have demonstrated a difference in the distribution of con A binding sites between normal and transformed or tumor cells. This difference was seen whether these cells were fixed or not prior to labelling with con A and when they were incubated in con A at different temperatures. Con A binding sites have been found to be evenly distributed in both normal and transformed cells when they were prefixed or if they were labeled with lectin at 4 °C. However, clustering or patching of con A binding sites in transformed or tumor cells was observed only when unfixed cells were exposed to lectin and incubated at 37 °C [3, 8, 9, 12, 13, 17, 19, 23]. On the other hand, some normal cells have con A binding sites in clusters and these cells show a dispersed distribution of the receptors at 37 °C incubation [7, 11, 22]. Thus, the distribution pattern of con A binding sites on the cell surface may differ according to the experimental condition and the types of cells. This study demonstrated the difference in the distribution and the density of con A binding sites between normal mucosa and bladder tumor under the experimental condition of prefixation and labelling at room temperature (15–25 °C).

Concerning the number of con A receptor sites, a study using a radiolabeled lectin demonstrated that there were several times more con A receptor sites on the transformed or tumor cell than on the normal cell [14, 21]. However, many studies show that normal cells do not differ significantly from transformed cells in the number of con A binding sites (review of [20]). Considerable controversy exists over the distribution and the number of con A binding sites on the cell surface of various cell types. Almost all of these results were obtained from the experiments at the free cell level and no studies have been done at the tissue level of tumor. In the present study, surface con A binding sites were more numerous in bladder tumor tissue than in the normal bladder mucosa as demonstrated by TEM, SEM and quantitative analysis with a X-ray microanalyzer, and these binding sites, moreover, increased in number in proportion to the grade of the tumor. These con A binding reactions may be specific to the con A binding sites, although some degree of non-specific binding may occur in the complicated spaces between many microvilli on the surface

of high grade bladder tumor, since con A binding to the receptors on the cell surface was inhibited by the addition of 0.2 M α-methyl-D-mannoside.

The other observations of con A binding to bladder urothelium showed that the superficial cells of the rat bladder were bound to con A [26] and normal human urothelium obtained by biopsies was stained by fluorescein isothiacyanate conjugated con A [1]. Neoplastic human urothelium has also been reported to be bound to con A [26], although the grade of tumor was unknown and no quantitative study was done. Increased agglutinability by con A was noted in rat isolated bladder epithelial cells exposed to carcinogens [15, 16]. This observation suggests that the increased agglutinability may be correlated to the appearance of microvilli in the urothelial cells. The present study demonstrated that the increased binding of con A occurred on the whole bladder epithelial surface independently of the appearance of microvilli during malignant transformation.

The investigation of lectin-resistant cell lines in cell culture suggested that cell-surface carbohydrate components are involved in certain adhesive, morphogenetic and metastatic phenomena [6].

It is generally recognized that a direct relation exists between bladder tumor grading and invasion or metastasis. The quantitative changes of con A binding in different bladder tumor grades may be associate with the biological potential for invasion or metastasis.

References

1. Alroy J, Szoka FC, Heaney JA, Ucci AA (1982) Lectins as a probe for carbohydrate residues in non-neoplastic urothelium of human urinary bladder. J Urol 128:189–193
2. Baccetti B, Burrini AG (1977) Detection of concanavalin A receptors by affinity to peroxidase and iron dextran by scanning and transmission electron microscopy and X-ray microanalysis. J Mircosc 109:203–209
3. Berlin RD (1975) Microtubular proteins and concanavalin A receptors. Adv Exp Med Biol 55:173–186
4. Bernhard W, Averameas S (1970) Ultrastructural visualization of cellular carbohydrate components by means of concanavalin A. Exp Cell Res 64:232–236
5. Bretton R, Clark DA, Nathanson L (1973) The cytochemical detection of concanavalin-A binding on cell surface by scanning electron microscopy. J Microsc 17:93–96
6. Briles EB (1982) Lectin-resistant cell surface variants of eukaryotic cells. Int Rev Cytol 75:101–165
7. Collard JG, Temmink JHM, Smets LA (1975) Cell cycle dependent agglutinability, distribution of concanavalin A binding sites and surface morphology of normal and transformed fibroblasts. Adv Exp Med Biol 55:221–244
8. De Petris S, Raff MC, Malluci L (1973) Ligand-induced redistribution of concanavalin A receptors on normal, trypsinized and transformed fibroblasts. Nature (London) New Biol 244: 275–278
9. Garrido J, Burglen MJ, Samolyk D, Wicker R, Bernhard W (1974) Ultrastructural comparison between the distribution of concanavalin A and wheat agglutinin cell surface receptors of normal and transformed hamster and rat cell lines. Cancer Res 34:230–243
10. Goldstein IJ, Hollerman CE, Smith EE (1965) Protein-carbohydrate interaction. II. Inhibition studies on the interaction of concanavalin A with polysaccharides. Biochemistry 4:876–883
11. Huet C, Bernhard W (1974) Difference in the surface mobility between normal and SV 40-, polyoma- and adenovirus- transformed hamster cells. Int J Cancer 13:227–239
12. Inbar M, Bassat BM, Sachs L (1973) Temperature-sensitive activity on the surface membrane in the activation of lymphocytes by lectins. Exp Cell Res 76:143–151
13. Inbar M, Huet C, Oseroff AR, Bassat BM, Sachs L (1973) Inhibition of lectin agglutinability by fixation of the cell surface membrane. Biochem Biophys Acta 311:594–599
14. Inbar M, Sachs L (1969) Structural difference in sites on the surface membrane of normal and transformed cells. Nature 223:710–712
15. Kakizoe T, Kamatsu H, Niijima T, Kawachi T, Sugimura T (1980) Increased agglutinability of bladder cells by concanavalin A after administration of carcinogens. Cancer Res 40:2006–2009
16. Kakizoe T, Kawachi T, Okada M (1978) Concanavalin A agglutination of bladder cells of rats treated with bladder carcinogens; A rapid new test to detect bladder carcinogens. Cancer Lett 285–290
17. Marikovsky T, Inbar M, Danon D, Sachs L (1974) Distribution of surface charge and concanavalin A-binding sites on normal and malignant transformed cells. Exp Cell Res 89:359–367
18. Martin BJ, Spicer SS (1974) Concanavalin A-iron dextran technique for staining cell surface mucosubstances. J Histochem Cytochem 22:206–209
19. Nicolson GL (1973) Temperature-dependent mobility of concanavalin A sites on tumour cell surfaces. Nature (London) New Biol 243:218–220
20. Nicolson GL (1974) The interactions of lectins with animal cell surfaces. Int Rev Cytol 39:89–190
21. Noonan K, Burger MM (1973) Binding of [^{3}H] concanavalin A to normal and transformed cells. J Biol Chem 248:4286–4292
22. Smith SB, Revel JP (1972) Mapping of concanavalin A binding sites on the surface of several cell types. Dev Biol 27:434–441
23. Temmink JMK, Collard JG, Spites H, Roos E (1975) A comparative study of four cytochemical detection methods of concanavalin A binding sites on the cell membrane. Exp Cell Res 92:307–322
24. Ukena TE, Borysenko JZ, Karnovsky MJ, Berlin RD (1974) Effects of colchicine, cytochalasin B and 2-deoxyglucose on the topographical organization of surface-bound concanavalin A in normal and transformed fibroblasts. J Cell Biol 61:70–82
25. Weller NK (1974) Visualization of concanavalin A-binding sites with scanning electron microscopy. J Cell Biol 63:699–707
25. Yokoyama M (1980) An electron microscopic study on the lectin-binding sites and their mobility in human and rat urologic tumor cells. Acta Histochem Cytochem 13:139–153

H. Takayama
Department of Urology
Shiga University of
Medical Science
Seta Tsukinowa
Otsu, 520–21
Japan